Journal of Integrative Neuroscience, Vol. 12, No. 4 (2013) 475–489

DOI: 10.1142/S0219635213500295

Imperial College Press
www.icpress.co.uk

Electromagnetic induction between axons and their schwann cell myelin-protein sheaths

G. Goodman* and D. Bercovich†,‡,§

*Galil Genetic Analysis, Kazerin 12900, Israel

†Faculty of Life Sciences, Tel-Hai College, Galilee 12210, Israel

‡Human Molecular Genetics and Pharmacogenetics
Migal Biotechnology Institute
Galilee, Kiryat Shmona 11016, Israel
§danib@migal.org.il

[Received 16 July 2013; Accepted 30 September 2013; Published 13 November 2013]

Two concepts have long dominated vertebrate nerve electrophysiology: (a) Schwann cell-formed myelin sheaths separated by minute non-myelinated nodal gaps and spiraling around axons of peripheral motor nerves reduce current leakage during propagation of trains of axon action potentials; (b) "jumping" by action potentials between successive nodes greatly increases signal conduction velocity. Long-held and more recent assumptions and issues underlying those concepts have been obscured by research emphasis on axon-sheath biochemical symbiosis and nerve regeneration. We hypothesize: mutual electromagnetic induction in the axon-glial sheath association, is fundamental in signal conduction in peripheral and central myelinated axons, explains the *g*-ratio and is relevant to animal navigation.

Keywords: Electromagnetic induction; neuron; axon; glial; myelin; sheath; *g*-ratio; node; paranode; internode.

1. Introduction

1.1. *The Schwann cell sheath*

In the vertebrate peripheral nervous system (PNS), numerous Schwann cells each wind a continuous, relatively compact, multi-layered spiral sheath of cell outer membrane around each motor axon. The non-myelinated gap (node) between each sheath is minute (~ 0.5–$2\,\mu$m), relative to internode length (~ 0.5–1.5 mm). This modified mainly lipid, bimolecular membrane, embedded with an asymmetric mosaic of proteins is doubled back, bringing its extracellular side into apposition with itself and similarly, the intracellular cytoplasm side with itself in a sandwich from between which the cytoplasm is squeezed out (Fig. 1).

The sheath was once regarded as protective, later as minimizing axon current leakage, insulation favoring signaling by propagation along motor axons of distally

§Corresponding author.

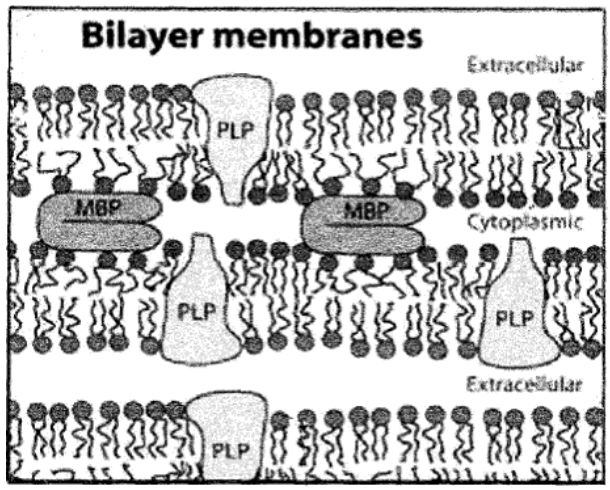

Fig. 1. Cross-section of a multi-layered, spiral myelin axon sheath. A doubling back of the outer side of glial cell membrane encloses extracellular space, alternatively with embrace of the cytoplasmic space by doubling back of the inner side of the cell membrane. The cytoplasmic space is shown stabilized by adhesion protein, myelin basic protein (MBP), compared to the more fluid, aqueous extra-cellular gap. The lipid bilayers are bridged by proteo-lipid-proteins (PLP) which differ between the peripheral and central nervous systems (CNS) (With kind permission of PNAS; Min *et al.*, 2009).

moving waves of transient, all-or-nothing, depolarization of the membrane potential (Fig. 2(a)). In the 40's and 50's, research suggested insulation restricted the repetitive excitation in a node-to-node "jumping" (saltatory) process (Fig. 2(b)) increasing conduction velocity. Since then, many assumptions and issues relating to the origin and nature of myelinated axon function remain unclarified as is evident in reviews of embryonic development, membrane composition, structure and function of glial cells and their association with axons (Jain, 1972a,b; Bunge *et al.*, 1989; Brown, 2003; Corfas *et al.*, 2004; Sherman & Brophy, 2005; Jessen & Mirsky, 2005; Quarles *et al.*, 2006; Court *et al.*, 2008; Ndubaku & Bellard, 2008; Debanne *et al.*, 2011).

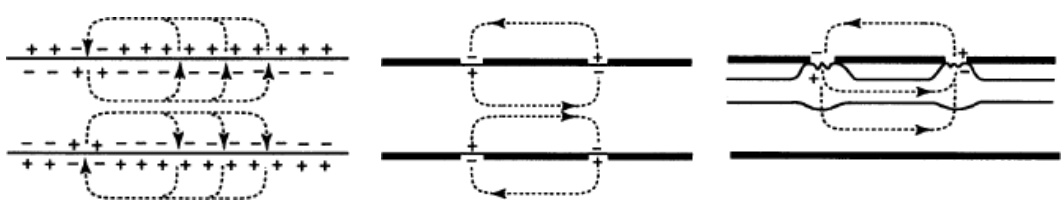

(a) (b) (c)

Fig. 2. (a)–(c). Models (not to scale) of local action current circuits during impulse conduction: (a), "rolling along" in a non-myelinated nerve fiber; (b), "jumping" along in a vertebrate myelinated nerve fiber; (c), "jumping" along in a shrimp myelinated nerve fiber. Thin continuous lines in (a) represent axon membrane, in (c), axon encased with inner sheath. Thick continuous lines in (b) represent axon spiraled with node-bearing myelin sheath, in (c), outer fenestrated myelin sheath. As common the diagrams do not show extra-cellular circuit return routes (Reproduced/adapted with permission; Xu & Terakawa, 1999).

1.2. *The sheath: Insulation questioned*

The sheath as insulator has long been debated (Jain, 1972b; Blight, 1985). Resistance of 260 myelin lamellae in the Goldfish Mauthner cell, was controversially reported as a third of that across the internode axolemma, questioning the influence of sheath thickness on signal propagation. Similarly, velocity was reported to vary with internode length, independent of myelin thickness (Funch & Faber, 1984), even though the common view that the ratio of sheath thickness to axon diameter expresses sheath resistance optimal for conduction predicts the same relation between sheath thickness and internode length, if axon diameter remains constant (Friede, 1986).

Similar electrophysiological thought and research on the PNS continues to depend on *in vitro* data, limitations on human experimentation, inconsistent clinical translation of experimental findings, well-rooted often conflicting approximations and assumptions such as fixed axonal and extra-axonal ion concentrations and ratios (Hodgkin & Huxley, 1952; Jain, 1972b; van Egeraat & Wikswo, 1993) and anatomic uncertainties such as those concerning the action circuit return route (Huxley & Stampfli, 1949; Friede, 1986) and the nature and function of the periaxonal gap.

However, older issues and more recent biophysical developments, such as evidence that solitons (a form of acoustic waves) travel rapidly along neuron membranes and are responsible for nervous signaling (Heimburg & Jackson, 2005), increasingly disturb classical positions. So too may innovation of particular interest in the context here: cable theory that incorporates Maxwellian considerations and allows in central dendrites intracellular membrane excitement moving as a continuum (and so signaling) along through fields associated with changing intracellular protein charge and polarization (Poznanski & Cacha, 2012). However, in axons the magnetic field is stronger than the magnetic field in dendrites because of the greater ionic currents flowing inside the axoplasm.

1.3. *The sheath: Roles and cost*

Sheaths are complex and costly, yet non- and barely myelinated fibers survive absence of "protection", while transfer between Schwann cell and axon e.g., of molecules and ribosomes (Court *et al.*, 2008) is not simplified by them. Schwann cell number per axon is unchanged from embryo to adult, so the maturing sheath elongates × 4 while diameter increases proportionally (Court *et al.*, 2004). Moreover, myelin layers must slide over each other (Inouye & Kirschner, 1988a) while maintaining relative stability. Sheath maturation is costly, yet saltatory conduction is commonly thought cheaper than unmyelinated conduction, as less energy is used to expel Na^+ from the axon. However, though inertness is historically accorded to "compacted" myelin lamellae, Schwann cells exhibit the energy-requiring cellular electro-sensitivity and maintenance requirements of all cells — unlikely to be lessened in their doubled-back, multi-layered, rolled-up myelin derivation. Recently

it was shown that energy for sheath production, maintenance and operation in CNS white matter, costs more than energy saved by "jumping" of action potentials (Harris & Attwell, 2012). Do the sheath roles identified to date, warrant alone the cost of the axon-sheath partnership?

1.4. *The axon: Crowded road in a charged atmosphere*

Transport along long PNS motor axons, is key to their existence and function. The axon is crowded with entities varying in size, complexity, stability and transience including microtubules, neurofilaments, ribosomes, mitochondria, vesicles, ions, transmitters and amino-acids. Traffic flows with almost equal bi-directionality, intermittent, asymmetric reversals of direction and variation in speed and rest periods up to 90% of the time (Brown, 2003). Traffic randomness alongside molecular motoring on fixed channels and highly synchronized, radial and bi-directional transfer of ions through innumerable membrane voltage gates (mostly at the nodes) are in an environment suffused with charge and polarity.

Microtubule formation is accompanied by substantial changes of charge distribution within tubulin subunits (Stracke *et al.*, 2002), tubulin heterodimers have a permanent electric dipole (Ramalhoa *et al.*, 2006), almost 100% of the axonal microtubules of cat postganglionic sympathetic fibers had similar polarity orientation (Heidemann *et al.*, 1981), the shape and rigidity of axon microtubules is dependent on dipole–dipole interactions (Schoutens, 2005), neurofilaments with similar charge mutually repel and microtubules and filamentous actin can carry charge in ionic waves of a velocity similar to conduction in some nerves (Tuszynski *et al.*, 2004). The axon has always been regarded as an electrophysiological unit, however not because of its magnetic fields.

1.5. *Nerve magnetic fields: The poor relations?*

The living world is replete with electric fields (Pohl, 1973; Nuccitelli, 1992; Zhao *et al.*, 1999; Levin, 2003; McCaig *et al.*, 2009). Natural or applied, they interact in adjacent neurons (Katz & Schmitt, 1940), influence direction/rotation of growth cone neurites (Patel & Poo, 1982; Rajnicek *et al.*, 2006), regulate microtubules (Alvarez & Ramirez, 1979) and stimulate axon amino-acid uptake (Eugenin & Alvarez, 1995) and direct faster neurite growth towards cathodes than anodes (Jaffe & Poo, 1979). However, post-Faraday and reports of magnetic fields arising from steady body (Cohen *et al.*, 1980) and circuit currents (Barach *et al.*, 1985), in a recent relevant review "electric" appears 159 times, "magnetic" not once and in a modern neuroscience text, magnetism is indexed only under imaging and encephalic wave measurement. Yet magnetic fields have been measured by Wikswo *et al.* (1980) who measured the magnetic field strength to be 1.2×10^{-10} T for large frog sciatic nerve (with diameter of 0.6 mm) and reported as found by MRI in the brain (Xiong *et al.*, 2003).

2. A Heuristic Hypothesis

2.1. *Mutual electromagnetic induction between motor axons and their Schwann cells*

We hypothesize that magnetic fields and electric fields are mutually induced and functional within the axon-Schwann cell symbiosis. This physical relationship between vertebrate motor axons and the membranous sheaths spiraled around them, is a result of heavily charged and bi-directional axon flow, trans-axon membrane ion transfer, especially at nodes, and charged flow spiraling within the myelin lamellae. Moreover, Schwann cell and sheath-induced magnetic fields in each of the node, paranode and internode regions separately, influences axon charge, polarity, structure, transport, viscosity, content and flow. This increases efficiency and velocity of the trains of node–node action circuits.

2.2. *Mutual induction — A recall in short*

A varying current of electrons, ions, charged molecules or particles moving through a conductor (e.g., axon-based), induces a first (primary) magnetic field. Current is induced in a coiled circuit (here, the myelin sheath) immersed in the primary magnetic field which is changing in direction, velocity or magnitude (due to variations in its axon source). The induced spiral current induces a secondary magnetic field experienced by charged particles moving through it (here, in the axon) as a force at right angles to the direction of the particles and of the field. The force is due to interaction between the secondary field and the field arising from motion of the charged particles and its magnitude depends on velocity and charge of the particles and strength of the experienced field. The enforced direction of the particles, combined with that of the axial flow, can cause helical particle movement.

3. The PNS Myelinated Axon: An Electromagnetic-Physiological Unit

3.1. *Sheath gyral direction*

Sheath gyral direction was reported to be random (Bunge *et al.*, 1989), yet Schwann cells attaching to embryonic axons rotating uni-directionally towards their targets presumably gyrate similarly. Usually unconsidered, consistent direction of sheath helicity has been reported (Heacock & Agranoff, 1977; Tamada *et al.*, 2010), may have a role in induction but will not be considered further here.

3.2. *Induction: The paranode*

An obvious effect of the primary, axon-induced magnetic field on the sheath, is induction of currents of ions and charged particles circling the paranode in two cytoplasm-filled tubes formed by relaxed compaction between the cytoplasm faces of myelin membrane at the two lateral edges of sheaths. Tube length varies with myelin turns. Each successive turn is adjunct with the axon and contiguous with its

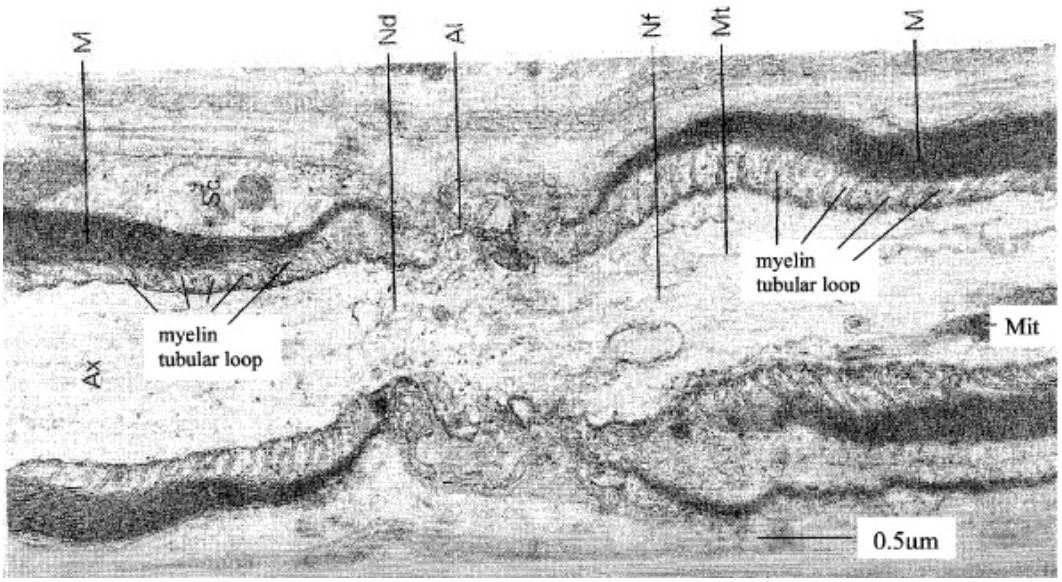

Fig. 3. Electron micrograph, longitudinal section through node–paranode region of PNS myelinated axon. All the cytoplasm-containing loops contacting the axolemma on both sides of the axon at one of its two edges, are part of single tube spiraling the axon. The other edge of each of the two part sheaths here is not shown. Node constriction is evident. Ax = axon; Sc = Schwann cell body; M = myelin-protein sheath; Nd = node; Nf =neurofilament; Al = axolemma; Mt = microtubule; Mit = mitochondrion (By kind permission of Oxford University Press; Peter *et al.*, 1991).

neighbors, the outermost with a node (Fig. 3)]. A lateral tube of one internode is distal to, and one from a neighboring internode proximal to a given node. Tube adjunctions with an axon were long considered as preventing sub-internode transmembrane axon current from reaching the paranode/nodal space. Recent evidence negates that (Mierzwa *et al.*, 2010), questioning multiple seals when a few would seem adequate. However, charge moving around many tube turns supports induction of a secondary magnetic field influencing intra-axon content and transport. For example, disturbance of induction by demyelination may have affected charges on, so alignment of long polymers and transport critical generally for regeneration in Trembler mice (de Waegh & Brady, 1990).

Current return from induced paranode spiral circuits, may relate intranode length with conduction velocity. Return to the Schwann cell body may be via intra-sheath gap junctions (Balice-Gordon *et al.*, 1998), but more likely it is through cytoplasm bands of Cajal external to the sheath (Ushiki & Ide, 1987; Court *et al.*, 2004). Internode shortening accompanying reduced conduction velocity in mutant Schwann cells, was thought due to depleted nutrition caused by absence of longitudinal Cajal bands (Court *et al.*, 2004). However, reduced velocity may result from weakened induction due to their absence. Similarly, slower conduction when internode length is beyond optimum (Brill *et al.*, 1977) would result from fewer paranode tubes, so weaker induction. Remarkably, impulse conduction was slowed more by paranode

demyelination than by uniform demyelination of an entire internode (Koles & Rasminsky, 1972), suggesting criticality of induction at the paranode and perhaps at the node too.

3.3. *Induction at the node*

The primary magnetic field induces spiraling around a node of the charged content of two rings of Schwann cell cytoplasm, one each side of the node. This induces a secondary magnetic field independent of and unlike that of the paranode. In clinical research on how to indirectly measure action potentials, the magnetic field of a propagating non-saltatory axon circuit (Fig. 4) was found to reverse direction with depolarization/repolarization of the action potential (Wijesinghe, 2010). In saltatory propagation, reversal of potential is nodal; as is reversal of field direction. This may reduce problems caused by node constriction.

3.3.1. *Induction at the node: Constriction and blockage*

The tendency to blockage caused by constriction, is usually a little more proximal than distal in the node (Weiss & Pillai, 1965), due perhaps to greater anterograde than retrograde axon flow. It is proposed that primary magnetic fields at the node are strengthened by constriction-increased axon flow velocity, leading to faster flow of charged cytoplasm content encircling nodes and so to a secondary magnetic field that effects long, large, charged, polarized molecular structures in a manner causing a more orderly parallel flow through the constriction (see Fig. 3). Notably, slowing of impulse conduction was greatest when paranode demyelination was simulated on both sides of a node, least when it was only distal (Koles & Rasminsky, 1972),

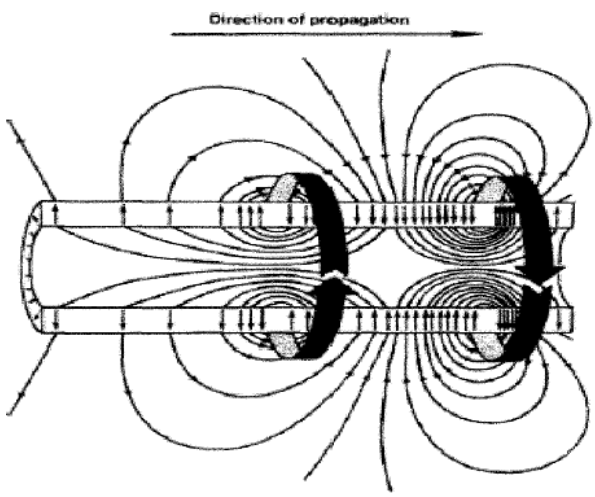

Fig. 4. Not-to-scale, axon cross-section showing direction of electric fields and associated magnetic fields (wide arrows) which were measured and related to action potential. Magnetic field directions alternate with those of the radial and linear currents (Reproduced by kind permission of IEEE, Piscataway, NJ; Wikswo, 1988).

supporting the presence of an independent, constriction-clearing process relatively unaffected in the unmyelinated node.

3.3.2. *Induction at the node: Constriction and viscosity*

Viscosity is generally problematic in axons. Doubled intracellular viscosity in a perfused squid giant axon more than doubled duration of action potential, halved rate of rise, increased resting membrane resistance by 60% and considerably slowed inward and outward currents, effects irrespective of some other biochemical and physical parameters, and is reversible (Kukita & Yamagishi, 1979). Lower viscosity aids elongation of a growing axon (O'Toole *et al.*, 2008) and increasing viscosity with age limits elongation of adult axons in growth and regeneration (Lamoureux *et al.*, 2010). Viscosity of some piped crude oils is attenuated by very short pulsed magnetic fields which improve flow downstream for some hours, perhaps by aggregation of micro-entities (Tao & Xu, 2006). Similar effect of rapidly-alternating, magnetic fields on axon viscous flow may persist to the next node.

3.4. *The internode*

In the early fifties and well after, the little known facts about the "compact", "inert" myelin sheath rested on a misleading cable analogy. The myelin sheath is a specially adapted myelin-protein structure, that undergoes dynamic equilibration between attraction and repulsion in its semi-fluidic, bi-layers. This particularly involves van der Waals attraction due to fluctuating charges and electrostatic repulsion due to concentration gradient of diffusible ions at a stable charged surface; also repulsive are hydration and membrane fluctuations out of plane: water in sciatic nerve sheath is above 40% adding considerable, non-covalent binding and fluidity (Inouy & Kirschner, 1988b). The relatively fused, apposition of cytoplasm membranes is stable due to MBP (Min *et al.*, 2008), the extracellular apposition is weakened by aqueous separation and both are influenced by pH and ionic strength. This effects extracellular periods and the surfaces carry a net negative charge varying with ionic strength. Relative invariance of cytoplasmic space and packing implies specific, short range interactions (Inouye & Kirschner, 1988a,b), and overall sheath function is linked by protein bridges (PLP) between its spaces (Fig. 1).

3.4.1. *The internode: Induction*

Clearly, the intra-sheath environment is charged and dynamic. Interesting here is a proposal that action current leaks not radially, trans-sheath, but around and through the water-rich, sheath extracellular membrane apposition (Friede, 1986). Internode anatomy sourcing secondary induction requires an axon-induced, primary magnetic field driving charge spirally within the internode, either sequentially in many independent, myelin-protein loop units, or as a single, long helical loop. Either way, the primary field induction would be response to sub-internode axon currents and the

secondary magnetic field source would be spiral cytoplasmic, or extracellular flow, or both independently differing in direction, time and magnitude.

3.4.2. *The internode: Induction and the axon*

Fuller appreciation of the dynamic interfaces between the sheath lamellae, may support internode secondary field criticality for the action potential and its "jumping" over the very long internode distances. Moreover, though some secondary effects on subinternode axon content and flow may be similar to those of the induced node and paranodal fields, they may differ. For example, in longitudinal axon flow the Lorenz force acting on a free particle would result in helical advance. Mitochondria were found close to the axolemma in large numbers and though thought possibly docked, large numbers were also found at the axon terminal (Weiss & Pillai, 1965). Free, helically-moving organelles close to the axolemma may keep them clear of fixed structures involved in mechanical transportation, much debated, very long, thin polymers and cytoskeleton generally.

The most inner sheath lamella was once incorrectly thought to wrap the axon tightly and that "transmission of the nervous impulse depends on currents flowing outside the myelin sheath" (Huxley & Stampfli, 1949). The electron microscope revealed between axon and sheath a subinternode, periaxonal space, physiologically not more than 30 nm wide (Trapp *et al.*, 1984) and remarkably stable even in some pathological conditions. Though currently regarded mainly as a sink for diffusion away of excess K^+, it may be of particular interest concerning putative internode induction, but outside the scope here, unlike the equally challenging *g*-ratio.

4. The g-Ratio Issue

4.1. *The g-ratio*

$$g\text{-ratio} = \text{axon diameter}/(\text{that diameter} + \text{double the thickness of the axon sheath}).$$

It has long been a critical parameter in research and debate on axon-sheath geometry and its relationship with conduction velocity and is consistently centered around 0.7 (CNS usually higher). Reported early as 0.6 (Rushton, 1951), Chomiak & Hu (2009) quote 12 reports giving ratios of 0.55 to 0.8 for different rat nerves: the (unreported) average is 0.68. *g*-ratios of phrenic nerves of seven differently aged groups of rabbits ranged from 0.59 to 0.73 (Friede *et al.*, 1985): unreported average, 0.67. Our recent blind measurements on undistorted, myelinated axon profiles in micrographs from two rodent species, published by separate laboratories and not intended for *g*-ratio measurement, demonstrate similar linear correlations ($p < 0.00001$) with average *g*-ratios of 0.68 ($n = 31$) and 0.7 ($n = 33$).

4.2. *g-ratio: Source*

Here, the ratio is rooted in the laws of electromagnetic induction: a biological benefit based on a non-adaptive physical "constant", not an advantage derived directly from natural selection of random genetic changes, though dependent on them for expression. The advantage most likely concerns conduction speed, is dependent on the magnetic flux at any time and point along a sheathed axon and expressed according to

$$\Phi = AB\cos\theta,$$

where Φ = magnetic flux, A = area of axon cross-section, B = magnetic field, θ = angle of inclination between the normal of the cross-sectional area of the axon and the direction of an axon-induced magnetic field. In nature, unlike in the laboratory, the axon is a very thin, long, flexible and undulating living structure influenced by a constantly changing internal and external physical and chemical environment. The angle between the field and the normal to the axon cross-sectional area at any point in space and time averages around 45° (cosine 0.7071). In the PNS in both vertebrates and some invertebrates, *g*-ratios range from 0.6 or less to over 7.0 according to physical and technical conditions, age and species. Brain *g*-ratios tend to 0.8 or more.

4.3. *g-ratio: An expression of the sheath-axon electromagnetic symbiosis*

Despite wide natural variation and artifact due to methodology and subjectivity, the data point to the *g*-ratio as a remarkable phenomenon long debated in relation to its relationship with internode length and conduction velocity (Hursh, 1939; Rushton, 1951; Smith & Koles, 1970; Arbuthnott *et al.*, 1980; Friede & Beuche, 1985; Friede *et al.*, 1985; Chomiak & Hu, 2009). The evidence suggests the axon is not alone or key in influencing sheath thickness and most agree the *g*-ratio is the most informative, consistent measure of sheath impact on axon function (Friede & Beuche, 1985). A common view (Chomiak & Hu, 2009) is that the ratio reflects evolution under spatial constraint and optimal metabolism. In addition to the mentioned findings of Harris & Attwell (2012), doubt is also thrown on that by some cold-blooded invertebrates.

5. On Sheaths and Shrimps

The fastest conduction known (up to 200 m/sec or more) and a *g*-ratio of 0.69±0.10 averaged across a wide size range in 110 myelinated fibers, have been found in some shrimp species (Fig. 2(c)) with fenestrations through the sheath (rather than nodes) to direct contact with a giant axon (Hsu & Terakawa, 1996; Xu & Terakawa, 1999). The axon is surrounded tightly by an inner sheath packed with long, straight micro-tubules parallel to its axis and encircled by other micro-tubules — mindful of the vertebrate spiraling sheath-axon structure, a comparison augmented by known

micro-tubule electrical characteristics. A further difference from vertebrates: between the tubules and a layered outer myelin sheath is a wide gel-filled sub-myelinic space (Fig. 2(c)) greatly lowering local circuit resistance (Xu & Terakawa, 1999) and weakening the argument that the similar *g*-ratio in vertebrates evolved due to spatial limitation. Notable too: despite the considerable anatomic differences between the shrimp and vertebrate sheaths, conduction velocity increased with axon diameter and sheath thickness as in vertebrates, though whereas vertebrate conduction usually varies with temperature, conduction was not slowed in the poikilotherms (Xu & Terakawa, 1999), weakening the argument that *g*-ratio ties directly to metabolism. Overall, these shrimps support electromagnetic induction in myelinated neurons and its archaic evolution.

6. Glial-Axon Electromagnetic Induction: Further Implications and Conclusion

If proved, the heuristic hypothesis of secondary, glial sheath-induced magnetic fields would have consequences peripherally and centrally beyond understanding of action potential propagation and relevant clinical motor issues. Proof will require fresh data and the considerable means for acquiring them from existing and perhaps newly developed experimental competencies. The need for detailed answers is perhaps a worthy challenge which hopefully may eventually advance knowledge of aspects of brain function. Answers may also point to a possible influence of ambient visible light which can penetrate vertebrate skulls at certain points, as measured using atlas-directed optic fibers in natural and artificial environments, (Goodman, 1983). As interaction between photons and magnetic fields has long been known and human life spans increase more rapidly than natural adaptation, how ambient light may interact, positively or negatively with postulated axon-glial sheath induced secondary magnetic fields would be of interest, especially as they would be more spatially diffuse than the well studied absorption of photons at specific loci (chromophores). Important too, would be interaction between geomagnetic and glial-axon, sheath-induced fields for animal navigation, especially in 3D environments, e.g., exceptionally long motor nerves of whales may also act as efficient direction and range finders. Though old questions are possibly answered here, new ones are raised. Nevertheless, one may be encouraged by the thought that it is not unlikely that the ubiquitous electromagnetic induction of today's technology was anticipated by natural selection of a glial sheath-axon symbiosis as now proposed.

Acknowledgments

We are much indebted to Prof. P. A. Riley (Cell Biology and Pathology, University College, London) for repeated reading and thoughtful and encouraging comments. We are grateful to Prof. R. S. Wijesinghe (Physics, Ball State University, Indiana) for reading and penetrating, helpful comments.

REFERENCES

Alvarez, J. & Ramirez, B.U. (1979) Axonal microtubules: Their regulation by the electrical activity of the nerve. *Neurosci. Lett.*, **15**, 19–22.

Arbuthnott, E.R., Boyd, I.A. & Kalu, K.U. (1980) Ultrastructural dimensions of myelinated peripheral nerve fibres in the cat and their relation to conduction velocity. *J. Physiol. (Lond)*, **308**, 125–157.

Balice-Gordon, R.J., Bone, L.J. & Scherer, S.S. (1998) Functional gap junctions in the Schwann cell myelin sheath. *J Cell Biol.*, **142**, 1095–1104.

Barach, J.P., Roth, B.J. & Wikswo, J.P. (1985) Magnetic measurement of action currents in a single nerve axon: A core conductor model. *IEEE Trans Biomed. Eng.*, **32**, 136–140.

Biondi, R.J., Levy, M.J. & Weiss, P.A. (1972) An engineering study of the peristaltic drive of axonal flow. *Proc. Nat. Acad. Sci. USA*, **69**, 1732–1736.

Blight, A.R. (1985) Computer simulation of action potentials and after-potentials in mammalian myelinated axons: The case for a lower resistance myelin sheath. *Neuroscience*, **15**, 13–31.

Brill, M.H., Waxman, S.G, Moore, H.J.W & Joyner, R.W. (1977) Conduction velocity and spike configuration in myelinated fibres: Computed dependence on internode distance. *J. Neurol.*, **40**, 769–774.

Brown, A. (2003) Axonal transport of membranous and non-membranous cargoes: A unified perspective. *J. Cell Biol.*, **160**, 817–821.

Bunge, R.P., Bunge, M.B. & Bates, M. (1989) Movements of the Schwann cell nucleus implicate progression of the inner (axon-related) Schwann cell process during myelination. *J. Cell Biol.*, **109**, 273–284.

Chomiak, T. & Hu, B. (2009) What is the optimal value of the g-ratio for myelinated fibers in the rat CNS? A theoretical approach. *PlosOne*, **4**, e7754.

Cohen, D., Palti, Y., Cuffin, B.N. & Schmid, S.J. (1980) Magnetic fields produced by steady currents in the body. *Proc. Natl. Acad. Sci. USA.*, **77**, 1447–1451.

Corfas, G., Velardez, M.O., Ko, C., Ratner, N. & Peles E. (2004) Mechanisms and roles of axon-schwann cell interactions. *J. Neurosci.*, **24**, 9250–9260.

Court, F.A., Hendricks, W.T.J., MacGillavry, H.D., Alvarez, J & van Minnen, J. (2008) Schwann cell to axon transfer of ribosomes: Toward a novel understanding of the role of glia in the nervous system. *J. Neurosci.*, **28**, 11024–11029.

Court, F.A., Sherman, D.L., Pratt, T., Garry, E.M., Ribchester, R.R., Cottrell, D.F., Fleetwood-Walker, S.M. & Brophy, P.J. (2004) Restricted growth of Schwann cells lacking Cajal bands slows conduction in myelinated nerves. *Nature*, **431**, 191–195.

Debanne, D., Campanac, E., Bialowas, A., Carlier, E. & Alcaraz, G. (2011) Axon physiology. *Physiol. Rev.*, **91**, 555–602.

de Waegh, S. & Brady, S.T. (1990) Altered slow axonal transport and regeneration in a myelin-deficient mutant mouse: The trembler as an *in vivo* model for Schwann cell-axon interactions. *J. Neurosci.*, **10**, 1855–1865.

Elder, G.A., Friedrich, V.L. & Lazarrini, R.A. (2001) Schwann cells and oligodendrocytes read distinct signals in establishing myelin sheath thickness. *J. Neurosci. Res.*, **65**, 493–499.

Eugenin, J. & Alvarez, J. (1995) Incorporation of amino acids into the axoplasm is enhanced by electrical stimulation of the fiber. *Brain Res.*, **677**, 319–325.

Friede, R.L. (1996) Relation between myelin sheath thickness, internode geometry, and sheath resistance. *Exp. Neurol.*, **92**, 234–247.

Friede, R.L. & Beuche, W. (1985) Combined scatter diagrams of sheath thickness and fibre calibre in human sural nerves: Changes with age and neuropathy. *J. Neurol. Neurosurg. Psychi.*, **48**, 749–756.

Friede, R.L., Brzoska, J. & Hartmann, U. (1985) Changes in myelin sheath thickness and internode geometry in the rabbit phrenic nerve during growth. *J. Anat.*, **143**, 103–113.

Funch, P.G. & Faber, D.S. (1984) Measurement of myelin sheath resistances: Implications for axonal conduction and pathophysiology. *Science*, **225**, 238–240.

Goodman, G. (1983) Light penetration of the cranium of the male domestic fowl in artificial and natural conditions. In: *Physiological Responses of the Cockerel to Light Quality: Growth and Sexual Development*. Ph.D. Thesis, Hebrew University of Jerusalem.

Hama, K. (1966) The fine structure of the Schwann cell sheath of the nerve fiber in the shrimp (Penaeus japonicus). *J. Cell Biol.*, **31**, 624–632.

Harris, J.J. & Attwell, D. (2012) The energetics of CNS white matter. *J. Neurosci.*, **32**, 356–371.

Heacock, A.M. & Agranoff, B.W. (1977) Clockwise growth of neurites from retinal explants. *Science*, **198**, 64–66.

Heidemann, S.R., Landers, J.M. & Hamborg, M.A. (1981) Polarity orientation of axonal microtubules. *J. Cell Biol.*, **91**, 661–665.

Heimburg, T. & Jackson, A.D. (2005) On soliton propagation in biomembranes and nerves. *Proc. Natl. Acad. Sci. (U.S.A)*, **102**, 9790–9795.

Hodgkin, A.L. & Huxley, A.F. (1952) A quantitative description of membrane current and its application to conduction and excitation in nerve. *J. Physiol. (Lond)*, **117**, 500–544.

Hsu, K., & Terakawa, S. (1996) Fenestration in the myelin sheath of nerve fibers of the shrimp: A novel node of excitation for saltatory conduction. *J. Neurobiol.*, **30**, 397–409.

Hursh, J.B. (1939) Conduction velocity and diameter of nerve fibers. *Am. J. Physiol.*, **127**, 131–139.

Huxley, A.F. & Stampfli, R. (1949) Evidence for saltatory conduction in peripheral myelinated nerve fibres. *J. Physiol.*, **108**, 315–339.

Inouye, H. & Kirschner, D. (1988a) Membrane interactions in nerve myelin: I Determination of surface charge from effects of pH and ionic strength on period. *Biophys. J.*, **53**, 235–245.

Inouye, H. & Kirschner, D. (1988b) Membrane interactions in nerve myelin: II Determination of surface charge from biochemical data. *Biophys. J.*, **53**, 247–260.

Jaffe, L.F. & Poo, M. M. (1979) Neurites grow faster towards the cathode than the anode in a steady field. *J. Exp. Zool.*, **209**, 115–128.

Jain, M.K. (1972a) Excitability: Time-dependent phenomena in membranes. In: *The Bimolecular Lipid Membrane.* New York: Van Nostrand Reinhold.

Jain, M.K. (1972b). Theories of action potential. In: *The Bimolecular Lipid Membrane.* New York: Van Nostrand Reinhold.

Jessen, K.R. & Mirsky, R. (2005) The origin and development of glial cells in peripheral nerves. *Nat. Rev. Neurosci.*, **9**, 671–682.

Katz, B. & Schmitt, O.H. (1940) Electrical interaction between two adjacent nerve fibers. *J. Physiol. (Lond.)*, **97**, 471–488.

Koles, Z.J. & Rasminsky, M. (1972). A computer simulation of conduction in demyelinated nerve fibres. *J. Physiol.*, **227**, 351–364.

Kukita, F. & Yamagishi, S. (1979) Slowing of the time course of the excitation of squid giant axons in viscous solutions. *J. Membrane Biol.*, **47**, 303–325.

Lamoureux, P.L., O'Toole, M.R., Heidemann, S.R. & Miller, K.E. (2010) Slowing of axonal regeneration is correlated with increased axonal viscosity during aging. *BMC Neurosci.*, **11**, 140–149.

Levin, M. (2003) Bioelectromagnetics in morphogenesis. *Bioelectromagnetics*, **24**, 295–315.

McCaig, C.D., Song, B. & Rajnicek, A.M. (2009) Electrical dimensions in cell science. *J. Cell Sci.*, **122**, 4267–4276.

Mierzwa, A., Shroff, S. & Rosenbluth, J. (2010) Permeability of the paranodal junction of myelinated nerve fibers. *J. Neurosci.*, **30**, 15962–15968.

Min, Y., Kristiansen, K., Boggs, J.M., Husted, C., Zasadzinski, J.A. & Israelachvilia, J. (2008) Interaction forces and adhesion of supported myelin lipid bilayers modulated by myelin basic protein. *Proc. Natl. Acad. Sci. USA.*, **106**, 3154–3159.

Ndubaku, U. & Bellard, M.E. (2008) Glial cells: Old cells with new twists. *Acta. Histochem.*, **110**, 182–195.

Nuccitelli, R. (1992) Endogenous ionic currents and DC electric fields in multicellular animal tissues. *Bioelectromagn. Suppl.*, **1**, 147–157.

O'Toole, M., Lamoureux, P. & Miller, K.E. (2008) A physical model of axonal elongation: Force, viscosity and adhesions govern the mode of outgrowth. *Biophys. J.*, **94**, 2610–2620.

Patel, N.B. & Poo, M.M. (1982) Orientation of neurite growth by extracellular electric fields. *J. Neurosci.*, **2**, 483–496.

Peters, A., Palay, S.L. & Webster, H. de F. (1991) *The Fine Structure of the Nervous System: Neurons and their Supporting Cells*, 3rd edn. New York: Oxford University Press, p. 249.

Pohl, H. (1973) Biophysical aspects of dielectrophoresis. *J. Biol. Phys.*, **1**, 1–16.

Poznanski, R. R & Cacha, L.A. (2012) Intracellular capacitive effect of polarized proteins in dendrites. *J. Integr. Neurosci.*, **11**, 417–438.

Quarles, R.H., Macklin, W.B. & Morell, P. (2006) Myelin formation, structure and biochemistry. In: G.J. Siegel, B.W. Agranoff, R.W. Albers and M.D. Molinoff, eds. *Basic Neurochemistry: Molecular, Cellular and Medical Aspects.* New York: Elsevier.

Rajnicek, A.M., Foubister, L.E. & McCaig, C.D. (2006) Growth cone steering by a physiological electric field requires dynamic microtubules, microfilaments and Rac-mediated filopodial asymmetry. *J. Cell Sci.*, **119**, 1736–1745.

Ramalhoa, R.R., Soaresb, H. & Melo, L.V. (2006) Micro-tubule behavior under strong electromagnetic fields. *Mat. Sci. Eng. C*, **27**, 1207–1210.

Rushton, W.A.H. (1951) A theory of the effects of fibre size in medullated nerve. *J. Physiol. (Lond.)*, **115**, 101–122.

Schoutens, J.E. (2005) Dipole–dipole interactions in microtubules. *J. Bio. Phys.*, **31**, 35–55.

Sherman, D.L. & Brophy, P.J. (2005) Mechanisms of axon ensheathment and myelin growth. *Nature Revs. Neurosci.*, **6**, 683–690.

Smith, R.S. & Koles, Z.J. (1970) Myelinated nerve fibres: Computed effect of myelin thickness on conduction velocity. *Am. J. Physiol.*, **219**, 1256–1258.

Stracke, R., Bohm, K.J., Wollweber, L., Tuszynski, J.A. & Ungera, E. (2002) Analysis of the migration behavior of single microtubules in electric fields. *Biochem. Biophys. Res. Commun.*, **293**, 602–609.

Tamada, A., Kawase, S., Murakami, F., Kamiguchi, H., Tamada, A., Kawase, S., Murakami, F. & Kamiguchi, H. (2010) Autonomous right-screw rotation of growth cone filopodia drives neurite turning. *J. Cell Biol.*, **188**, 429–441.

Tao, R. & Xu, X. (2006) Reducing the viscosity of crude oil by pulsed electric or magnetic field. *Energy & Fuels*, **20**, 2046–2051.

Trapp, B.D., Quarles, R.H. & Suzuki, K. (1984) Immunocytochemical studies of quaking mice support a role for the myelin-associated glycoprotein in forming and maintaining the periaxonal space and periaxonal cytoplasmic collar of myelinating schwann cells. *J. Cell Biol.*, **99**, 594–560.

Tuszynski, J.A., Portet, S., Dixon, J.M., Luxford, C. & Cantiello, H.F. (2004) Ionic wave propagation along actin microfilaments. *Biophys. J.*, **86**, 1890–1903.

Ushiki, T. & Ide, C. (1987) Scanning electron microscopic studies of the myelinated nerve fibres of the mouse sciatic nerve with special reference to the Schwann cell cytoplasmic network external to the myelin sheath. *J. Neurocytol.*, **16**, 737–747.

van Egeraat, J.M. & Wikswo, J.P. (1993) A model for axonal propagation incorporating both radial and axial ionic transport. *Biophys. J.*, **64**, 1287–1298.

Waxman, S. (1980) Determinants of conduction velocity in myelinated nerve fibers. *Muscle Nerve*, **3**, 141–150.

Weiss, P. & Pillai, A. (1965) Convection and fate of mitochondria in nerve fibers: Axonal flow as vehicle. *Proc. Natl. Acad. Sci.*, **54**, 48–56.

Wijesinghe, R.S. (2010) Magnetic measurements of peripheral nerve function using a neuromagnetic current probe. *Exp. Biol. Med.*, **235**, 159–169.

Wikswo, J.P. (1988) Magnetic techniques for evaluating peripheral nerve function. *Proc. 10th Ann. EMBS Conf.*, New Orleans, LA.

Wikswo, J.P., Barach, J.P. & Freeman, J.A. (1980) Magnetic field of a nerve impulse: First measurements. *Science*, **208**, 53–55.

Xiong, J., Fox, P.T. & Gao J. (2003) Directly mapping magnetic field effects of neuronal activity by magnetic resonance imaging. *Hum. Brain Mapp.*, **20**, 41–49.

Xu, K. (Hsu, K.) & Terakawa, S. (1999) Fenestration nodes and the wide submyelinic space form the basis for the unusually fast impulse conduction of shrimp myelinated axons. *J. Exp. Biol.*, **202**, 1979–1989.

Zhao, M., Forrester, J.V. & McCaig, C.D. (1999) A small, physiological electric field orients cell division. *Proc. Natl Acad. Sci. USA*, **96**, 4942–4946.